Electronic Supplementary Information

A six-bladed impeller-like Cu_{18} nanocluster with S_6 symmetry constructed from simple inorganic linkers

Zilu Chen,* Yifei Wang, Long Liu, Zhong Zhang, and Fupei Liang*

Table of content:

Experimental Details

Materials and General Methods

All chemicals were used as obtained without further purification. Infrared spectra were recorded as KBr pellets using a Nicolet 360 FT-IR spectrometer. Elemental analyses (C, H and N) were performed on a Vario EL analyser. The powder X-ray diffraction (PXRD) data were collected with a Rigaku D/max 2500v/pc diffractometer with Cu-Kα radiation (λ = 1.5418 Å). Thermogravimetric analyses were recorded with a NETZSCH TG 209F1 Iris analyzer at a rate of 10 °C/min from room temperature to 910 °C under a nitrogen atmosphere. All magnetic measurements (solid state) were carried out on a Quantum Design MPMS-XL SQUID magnetometer in a temperature range of 2.0–300 K and a DC field of 1000 Oe. Data were corrected for the diamagnetic contribution calculated from Pascal constants and the diamagnetism of the sample and sample holder were taken into account.

1. Synthesis of 2-(1-hydroxy-2-methylpropan-2-ylimino)-1,2-di-phenylethanone

An ethyl acetate or THF (50 mL) solution of benzyl (2.1 g, 10 mmol) and 2-amino-2-methyl-1-propanol (2.275 g, 25 mmol) in a 100 mL round-bottomed flask was refluxed at 80 °C for 20 hours. It was then cooled and separated by column chromatography, giving a white powdery product (2.4 g, 85.4%) after the removal of solvent. m.p. 150-153 °C; Found: C, 76.6; H, 6.5; N, 5.1; $C_{18}H_{19}NO_2$ requires: C, 76.8; H, 6.8; N, 5.0%; IR (KBr, cm^{-1}): ν_{max} = 3437 (s), 2973 (w), 2929 (w), 2863 (w), 1608 (m), 1443 (w), 1383 (w), 1265 (m), 1235 (w), 1185 (w), 1066 (s), 968 (w), 936 (w), 905 (w), 757 (w), 696 (m), 595 (w); ^{1}H NMR (500 MHz, $CDCl_3$): δ = 1.21 ppm (s, 3H, CH_3), 1.29 (s, 3H, CH_3), 3.61 (d, ^3J(H,H) = 8 Hz, 1H, CH_2), 3.90 (d, ^3J(H,H) = 8 Hz, 1H, CH_2), 7.28 (t, ^3J(H,H) = 7.4 Hz, 1H, Ph), 7.32 (t, ^3J(H,H) = 7.5 Hz, 2H, Ph), 7.35 (t, ^3J(H,H) = 7.5 Hz, 2H, Ph), 7.44 (t, ^3J(H,H) = 7.5 Hz, 1H, Ph), 7.61 (d, ^3J(H,H) = 7.5 Hz, 2H, Ph), 8.07 (d, ^3J(H,H) = 8 Hz, 2H, Ph); ^{13}C NMR (125.77 MHz, $CDCl_3$): δ = 25.8 (CH_3), 27.0 (CH_3), 59.4 (CH_2), 78.8 (CH_2), 125.3, 126.3, 127.7, 128.0, 128.1, 128.7, 121.5, 130.8, 132.8 (C=N), 197.4 ppm (C=O); MS (ESI): m/z 282.11 [M^+].

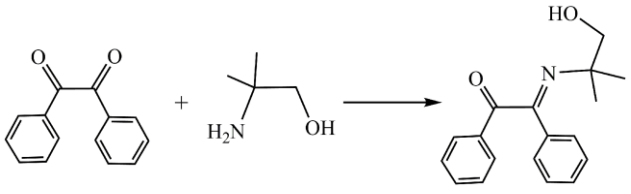

Scheme S1 A schematic show of the synthesis of 2-(1-hydroxy-2-methylpropan-2-ylimino)-1,2-di-phenylethanone

2. Synthesis of $[(HOCH_2)(CH_3)_2C(NH_3)]_{18}[Cu_{18}(SO_4)_{20}(OH)_{12}(DMF)_6](OH)_2\cdot 6DMF$ (1)

A mixture of 2-(1-hydroxy-2-methylpropan-2-ylimino)-1,2-di-phenylethanone (0.0562 g，0.2 mmol) and $CuSO_4\cdot 5H_2O$ (0.075 g，0.3 mmol) in DMF (4 mL) was sealed in a 25 mL Teflon-lined autoclave and heated at 60 °C in an oven for 5 days. Then it was allowed to be cooled to ambient temperature over 24 h, giving green crystals of **1** in a yield of 51%. Found: C, 22.1; H, 5.7; N, 7.35; S, 10.8; $C_{108}H_{314}Cu_{18}N_{30}O_{124}S_{20}$ requires C, 22.35; H, 5.45; N, 7.2; S, 11.05 %. IR (KBr, cm^{-1}): ν_{max} = 3116 (br), 2560 (w), 2016 (w), 1651 (s), 1594 (m), 1497(m), 1374(m), 1120 (vs), 1060 (s), 979 (m), 618 (s).

Attempted syntheses of 1 from 2-amino-2-methyl-1-propanol directly: A mixture of 2-amino-2-methyl-1-propanol (0.0178 g，0.2 mmol; or 0.0267 g, 0.3 mmol) and $CuSO_4\cdot 5H_2O$ (0.075 g，0.3 mmol) in DMF (4 mL) with the addition of 1 $mol\cdot L^{-1}$ H_2SO_4 (0.1 mL, 0.2 mL, 0.3 mL, 0.4 mL, 0.5 mL or 0.6 mL) was sealed in a 25 mL Teflon-lined autoclave and heated at 60 °C in an oven for 5 days. Then it was allowed to be cooled to ambient temperature over 24 h. An alternative method similar to the above one was also tried with the pH value of the reaction mixture controlled at 7, 6, 5, 4, 3, and 2 using 1 $mol\cdot L^{-1}$ H_2SO_4. Unfortunately, all of these attempts failed to give the targeted product as expected.

Discussion on the formation of $HOCH_2C(CH_3)_2NH_3^+$: The $HOCH_2C(CH_3)_2NH_3^+$ cations are the protonated form of 2-amino-2-methyl-1-propanol which is one of the starting materials for the synthesis of 2-(1-hydroxy-2-methylpropan-2-ylimino)-1,2-diphenylethanone. This means that the Schiff base of 2-(1-hydroxy-2-methylpropan-2-ylimino)-1,2-diphenylethanone underwent a decomposition process. In this reaction, the decomposition process of the Schiff base and the cluster formation process are synergistic. Presumably, the decomposition of the Schiff base into its corresponding materials might be triggered by the Cu(II) ions with the presence of water (which might be from $CuSO_4\cdot 5H_2O$ or the undried solvent) and air. For such possible mechanism, see "*Angew. Chem. Int. Ed.* **2012**, *51*, 3453–3457". Alternatively, the Schiff base in solution state with the presence of a small amount of water and air may undergo an equilibrium with largely towards the imine formation direction and the reverse process in a very low ratio. However, the cluster formation process leads to the protonation of 2-amino-2-methyl-1-propanol. Then the equilibrium is broken, leading to a completion of the reverse process.

X-ray crystallography.

The X-ray diffraction data of **1** was collected with Cu-Kα radiation (λ = 1.54178 Å). Absorption correction was applied by Empirical absorption correction using spherical harmonics, implemented in SCALE3 ABSPACK scaling algorithm. The structures were solved by direct methods using SHELXS-97 and refined by full-matrix least-squares against F^2 using the SHELXL-97 program. Full-matrix least-squares refinements on F^2, using all data, were carried out with anisotropic displacement parameters applied to all non-hydrogen atoms. H atoms attached to C atoms and N atoms were included in geometrically calculated positions using a riding model and were refined isotropically. H atoms on O atoms were located in difference Fourier maps and allowed for as riding on their parent atoms with U_{iso}(H) = 1.5U_{eq}(O). One SO_4^{2-} ion and the hydroxyl group of one $[(HOCH_2)(CH_3)_2C(NH_3)]^+$ cation were refined in a disordered manner. Some geometric restraints (EADP, DFIX and ISOR) were used in modeling the poor geometries of the $[(HOCH_2)(CH_3)_2C(NH_3)]^+$ cations, uncoordinated DMF molecules and the disordered SO_4^{2-} ions. Experimental details for the structure analysis of **1** are given in Table S1. The selected bond distances and angles for **1** are listed in Table S2.

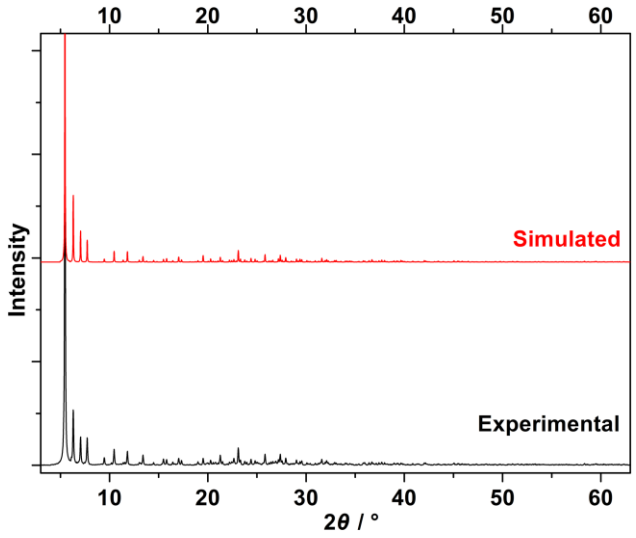

Fig. S1 Simulated and obtained PXRD pattern of **1**.

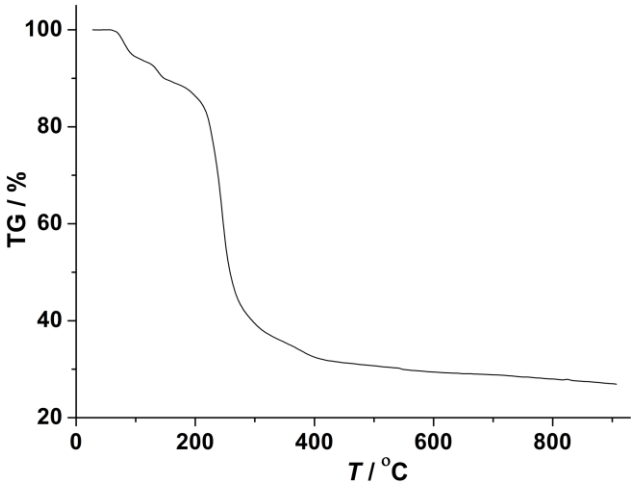

Fig. S2 TG curve of **1**. The weight loss of **1** started at 50 °C, which might be attributed to the loss of some $[(HOCH_2)(CH_3)_2C(NH_3)]^+$ cations or their decomposition products. This is consistent with that reported for $(HOCH_2)(CH_3)_2C(NH_2)$ in document (*Chem. Commun.*, 2010, **46**, 9158-9160). The followed was the loss of uncoordinated DMF and coordinated DMF and then the collapse of the skeleton. The final residue at 907 °C is 26.91%, which is close to the calculated value (24.67%) for CuO.

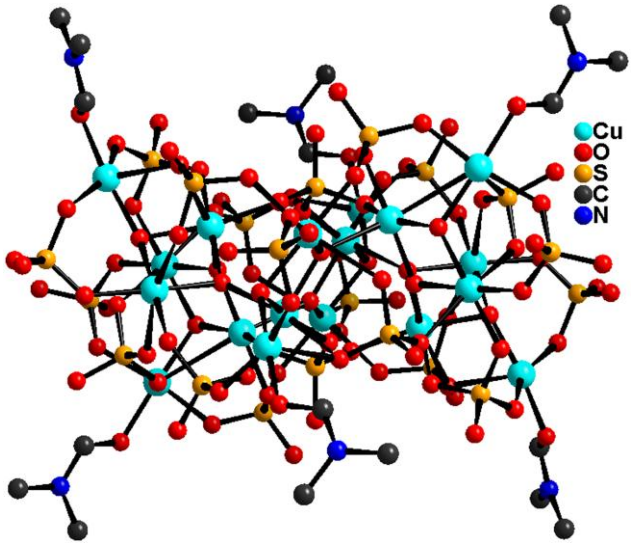

Fig. S3 A side view of the anionic cluster skeleton of $[Cu_{18}(SO_4)_{20}(OH)_{12}(DMF)_6]^{16-}$ in **1**.

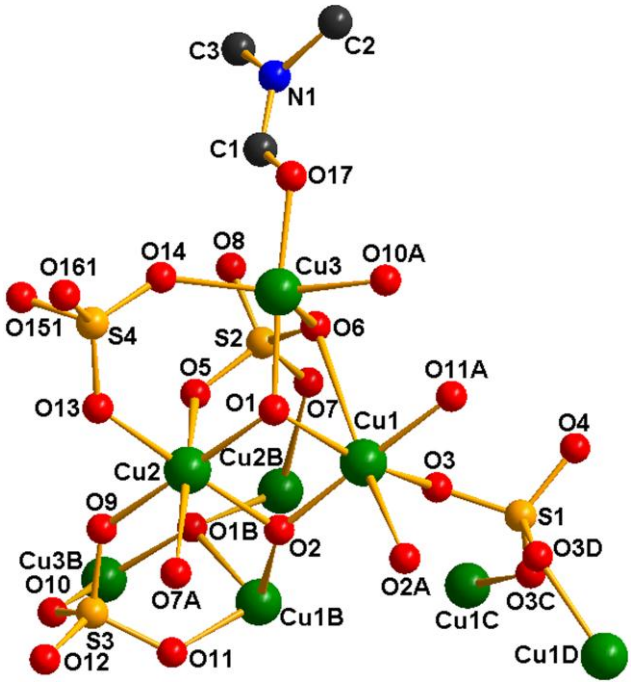

Fig. S4 A view of the coordination modes of Cu(II) ions and the bridging modes of the linkers of OH^- and SO_4^{2-} in **1** showing the atom-labeling scheme. Symmetry codes: A) $-z + 1, -x + 1, -y + 1$; B) $-y + 1, -z + 1, -x + 1$; C) y, z, x; D) z, x, y.

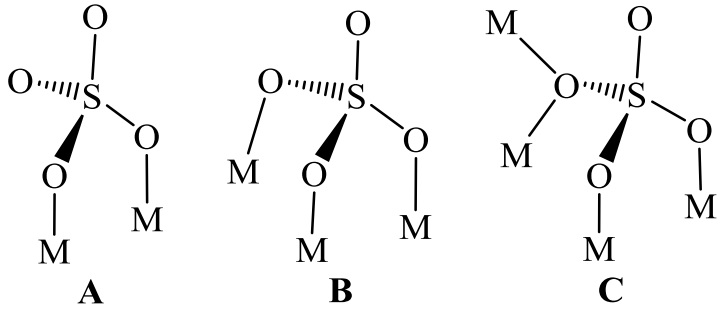

Scheme S2 A schematic show of the bridging modes of SO_4^{2-} ions in **1**.

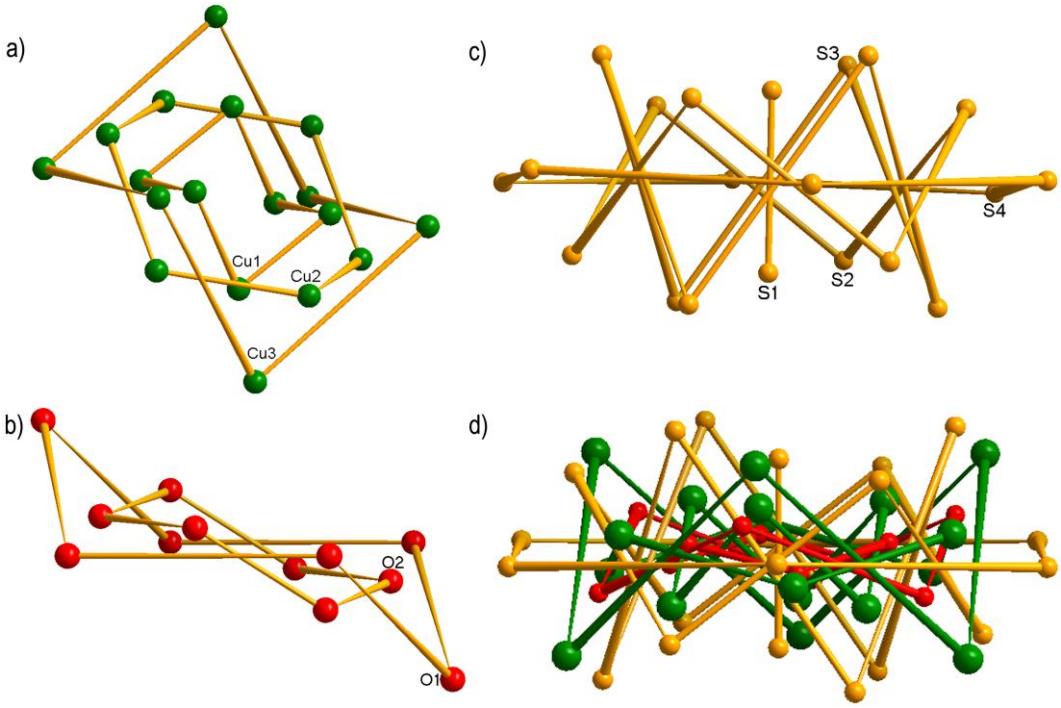

Fig. S5 A view of the arrangements of three groups of Cu(II) ions (a), two groups of OH^{-} ions (b) and four groups of SO_4^{2-} ions (c) and a side view of the arrangements of all Cu(II) groups and linker groups (d).

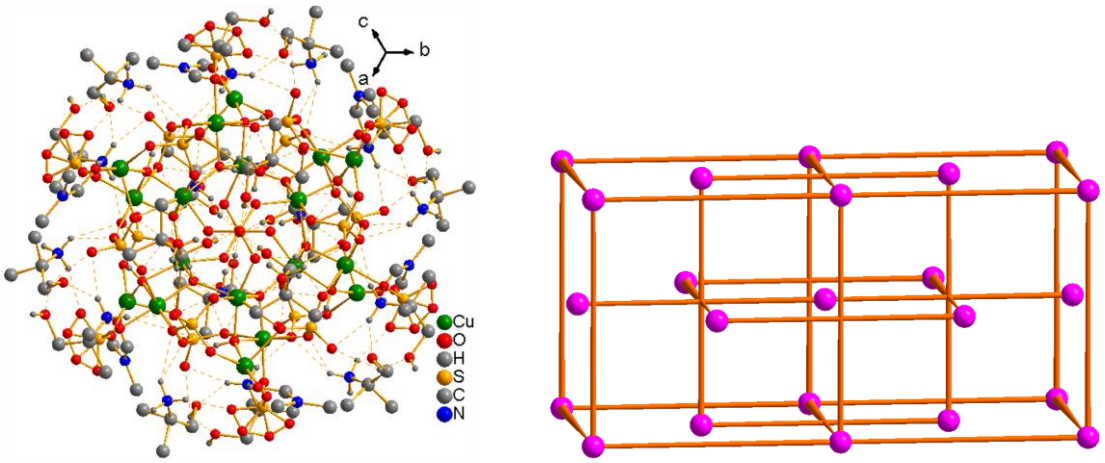

(a) (b)

Fig. S6 a) A view of the ball-like supermolecule formed by the $[Cu_{18}(SO_4)_{20}(OH)_{12}(DMF)_6]^{16-}$ ion and eighteen $[(HOCH_2)(CH_3)_2C(NH_3)]^{+}$ ions surrounded it by N-H···O hydrogen bonds; b) A packing-diagram of the supramolecular balls (purple spheres) of **1** in the lattice.

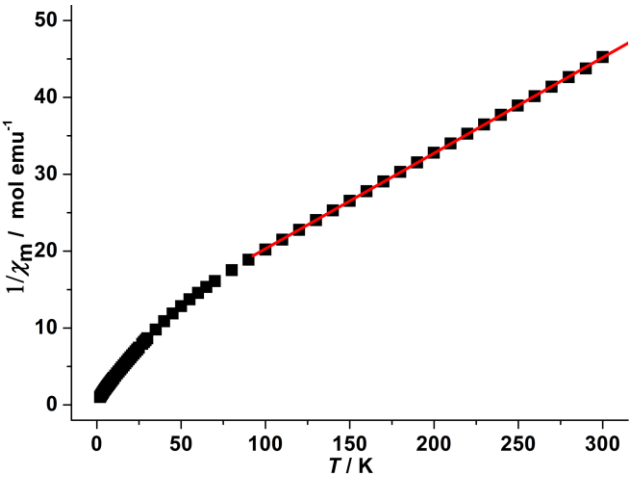

Fig. S7 The plot of χ_m^{-1} vs T for **1** in the temperature range of 2.0-300 K. The solid line represents the fitting by Curie-Weiss law in the temperature range of 100-300 K.

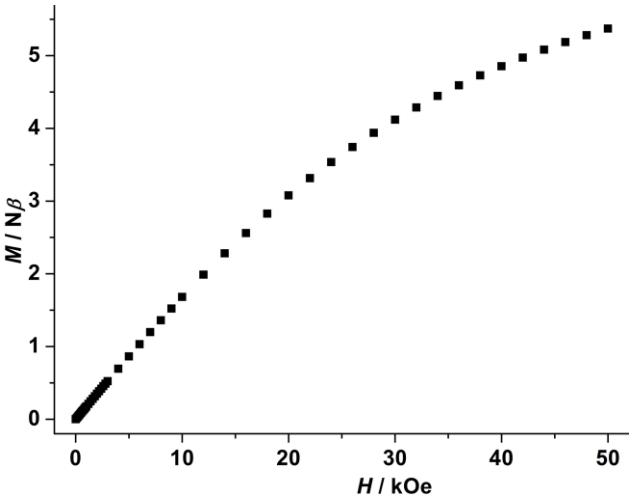

Fig. S8 Field dependence of the magnetization at 2 K below 50 kOe for **1**.

Table S1 Crystallographic data and structure refinement parameters for **1**.

formula	$C_{108}H_{314}Cu_{18}N_{30}O_{124}S_{20}$	F(000)	12024
fw	5802.81	Crystal size / mm	0.30 × 0.25 × 0.18
Temperature / K	161(2)	Limiting indices	$-21 \le h \le 32$
Wavelength / Å	1.54178		$-31 \le k \le 32$
Crystal system	Cubic		$-32 \le l \le 30$
Space group	*P*a-3	Reflections collected	76305
a / Å	28.00370(10)	Reflections unique	5936
b / Å	28.00370(10)	R_{int}	0.0618
c / Å	28.00370(10)	GOF on F^2	1.026
V / Å^3	21960.71(14)	R_1[a] ($I > 2\sigma(I)$)	0.0747
Z	4	wR_2[b] ($I > 2\sigma(I)$)	0.2050
D_c / g cm^{-3}	1.755	R_1[a] (all data)	0.0847
μ / mm^{-1}	4.566	wR_2[b] (all data)	0.2164
θ / °	3.16 to 63.72	Largest diff. peak and hole / e·Å^{-3}	0.994 and -0.846

[a] $R_1 = \Sigma\, ||F_o| - |F_c|| / \Sigma |F_o|$; [b] $wR_2 = [\Sigma w(F_o^2 - F_c^2)^2 / \Sigma w(F_o^2)^2]^{½}$.

Table S2 Selected bond lengths / Å and bond angles / º of **1**.

Cu1-O2	1.917(4)	Cu2-O2	1.936(4)	Cu3-O6	2.273(5)
Cu1-O11A	1.944(4)	Cu2-O13	1.946(5)	Cu3-O17	1.932(5)
Cu1-O1	1.965(4)	Cu2-O1	1.996(4)	Cu3-O1	1.930(4)
Cu1-O3	1.994(4)	Cu2-O9	1.996(4)	Cu3-O14	1.943(6)
Cu1-O2A	2.280(4)	Cu2-O7A	2.323(4)	Cu3-O10A	1.976(5)
Cu1-O6	2.712(4)	Cu2-O5	2.354(5)	O17-Cu3-O1	173.7(2)
O2-Cu1-O11A	178.41(18)	O2-Cu2-O13	176.5(2)	O17-Cu3-O14	88.3(2)
O2-Cu1-O1	84.38(17)	O2-Cu2-O1	83.07(16)	O1-Cu3-O14	95.1(2)
O11A-Cu1-O1	96.46(17)	O13-Cu2-O1	93.7(2)	O17-Cu3-O10A	84.1(2)
O2-Cu1-O3	92.38(15)	O2-Cu2-O9	97.27(17)	O1-Cu3-O10A	95.03(19)
O11A-Cu1-O3	87.31(16)	O13-Cu2-O9	85.9(2)	O14-Cu3-O10A	153.6(2)
O1-Cu1-O3	159.03(17)	O1-Cu2-O9	179.64(19)	O17-Cu3-O6	92.8(2)
O2-Cu1-O2A	94.04(11)	O2-Cu2-O7A	86.94(17)	O1-Cu3-O6	81.28(17)
O11A-Cu1-O2A	84.49(15)	O13-Cu2-O7A	91.7(2)	O14-Cu3-O6	102.3(2)
O1-Cu1-O2A	99.98(16)	O1-Cu2-O7A	93.27(17)	O10A-Cu3-O6	103.32(18)
O3-Cu1-O2A	100.92(15)	O9-Cu2-O7A	86.87(18)	Cu3-O1-Cu1	111.7(2)
O2-Cu1-O6	95.55(15)	O2-Cu2-O5	86.07(16)	Cu3-O1-Cu2	118.9(2)
O11A-Cu1-O6	86.01(15)	O13-Cu2-O5	95.9(2)	Cu1-O1-Cu2	93.88(18)
O1-Cu1-O6	69.94(15)	O1-Cu2-O5	97.12(16)	Cu1-O2-Cu2	97.39(17)
O3-Cu1-O6	89.84(14)	O9-Cu2-O5	82.79(18)	Cu1-O2-Cu1B	137.38(19)
O2A-Cu1-O6	165.27(13)	O7A-Cu2-O5	166.69(16)	Cu2-O2-Cu1B	117.41(17)

Symmetry codes: A) $-z + 1, -x + 1, -y + 1$; B) $-y + 1, -z + 1, -x + 1$.